Effect of Tin Addition on the Microstructure Development and Corrosion Resistance of Sintered 304L Stainless Steels

W.-F. Wang

(Submitted 10 June 1999; in revised form 17 August 1999)

The effect of tin powder addition on the microstructure development during sintering and corrosion resistance of the 304L-Sn metallurgical system was investigated. Specimens containing 1 to 4 wt% Sn were sintered in hydrogen at temperatures ranging from 800 to 1300 °C. During sintering at temperatures below 1000 °C, most of the liquid phase was retained at the site originally occupied by the tin powder. At temperatures above 1050 °C, the tin-base liquid phase spread and uniformly distributed among the 304L solid particles. Adding tin powder and the resultant liquid phase led 304L powder compacts to expand during sintering. An immersion test in 1 *M* H_2SO_4 and metallographic observation showed that pitting always initiated at the spots with lower tin content, and the tin atom enrichment had the beneficial effect of improving the corrosion resistance of sintered 304L stainless steels.

Keywords corrosion, powder metallurgy, sintering, tin addition, type 304 stainless steel

1. Introduction

The sintering behavior of iron powder compacts containing tin powder showed that 2 wt% Sn accelerates the sintering process considerably (Ref 1). The same strength can be obtained at lower sintering temperatures by adding tin rather than by adding copper powder. Previous work indicated that the sinterability of 304L stainless steel powder can be markedly improved by the addition of silicon powder, which induces liquid phase during sintering (Ref 2). The sintered density, mechanical properties, corrosion resistance, and high temperature oxidation resistance of sintered alloys also improved (Ref 3). The influence of a metallic element addition such as copper, tin, nickel, or molybdenum on various properties of sintered 304L stainless steels has been reported (Ref 4, 5). The effect of tin addition on the metallurgical properties of hot pressed and sintered 316L stainless steels has been investigated. The report shows that the amount of interconnected pores decreases by increasing the tin content, and the shape of pores changes from random to sphere (Ref 6). The corrosion resistance of these sintered alloys is similar to that of the wrought plate of type 316 stainless steel, and improvement of this property mainly resulted from decreasing the amount of interconnected pores, which is consequent upon the liquid phase sintering (Ref 7).

The purpose of the present article is to explore the microstructure development of 304L-Sn powder mixtures during sintering with a liquid phase. The effect of tin addition on the microstructure and the volume change of the mixed powder compacts was studied. The corrosion behavior of these sintered alloys in 1 *M* H_2SO_4 solution and the role of tin in improving the corrosion resistance were also investigated in detail.

W.-F. Wang, Department of Mechanical Engineering, Southern Taiwan University of Technology, Tainan, Taiwan.

2. Experimental Procedures

Water atomized stainless steel powder of the grade 304L was used. The particle size was –100 mesh. Table 1 gives the chemical composition and physical characteristics. The particle size of tin powder was –325 mesh. Batches of the 304L stainless steel powder were mixed with the tin powder (up to 4 wt%) in a three-dimensional rotating turbula-type mixer for 60 min. The powder mixtures were compacted in a single-acting hydraulic press at a pressure of 590 MPa. Cylindrical specimens, 11.35 mm in diameter and 5.0 mm in height, were used for metallographic examination, immersion testing, and measurement of green and sintered density and dimensional change after sintering. No lubricants were mixed with the powders, but a suspension of zinc stearate in acetone was applied to the die wall before powder filling. The compacts were sintered in the bottled hydrogen (dew point of –25 °C) at a temperature ranging from 800 to 1300 °C for 40 min.

The potentiodynamic polarization measurement was conducted in the 1 *M* sulfuric acid solution. The polarization curve was determined by using a PAR 273 potentiostat at a scan rate of 60 mV/min with all potentials referenced to a saturated calomel electrode. Immersion testing was also conducted to measure the corrosion rates of the sintered alloys. The weight loss during a testing period of 576 h was used to calculate the corrosion rates.

Table 1 Material composition and properties of AISI 304L stainless steel powder

Composition, wt%				Apparent density,	Flow rate,
C	Si	Cr	Ni	g/cm^3	50 g
0.02	0.9	18.8	10.9	2.7	31

3. Results and Discussion

3.1 Microstructure Development during Sintering

Figure 1(a) is an optical micrograph of 304L-Sn powder compacts sintered at 850 °C. Tin powder particles completely melt and form liquid pools. The liquid phase penetrates the particle boundaries, which possess higher free energy. Figure 1(b) shows the specimens sintered at 950 °C, in which the tin-base liquid phase further penetrates into the grain boundaries of a elliptic particle. This particle will disintegrate gradually and melt into the liquid phase. These phenomena can always be found in the initial stage of liquid phase sintering (Ref 2). Figure 1(c) displays the specimens sintered at 1050 °C. It shows a microstructure considerably different from those sintered below 1000 °C. In Fig. 1(a) and (b) most of the liquid phase is localized at the site originally occupied by the tin powder; it then gradually penetrates the 304L particle boundaries.

Above 1050 °C the wettability of solid particles by the liquid phase is greatly improved so that the liquid spreads all over within the specimens. The 304L particles are uniformly coated with a thin film of liquid phase. A similar situation has also been found in the investigation of sintering of 304L-Si powder mixtures (Ref 2). In the 304L-Si system only, when the sintering temperature is higher than 1100 °C, the eutectic liquid induced from contact melting of silicon powder can spread uniformly among the 304L particles.

Upon increasing the sintering temperature atoms of the liquid phase diffuse into the solid powder matrix, the thickness of liquid film gradually decreases. The characteristics of powder aggregates vanish, and the grain structure appears. Figure 1(d) shows a well sintered alloy at 1200 °C, in which the powder compact has been transformed into a polycrystalline solid. Due to intense diffusing of liquid atoms into the solid matrix the liquid phase disappears completely from the grain boundaries. A similar result has also been

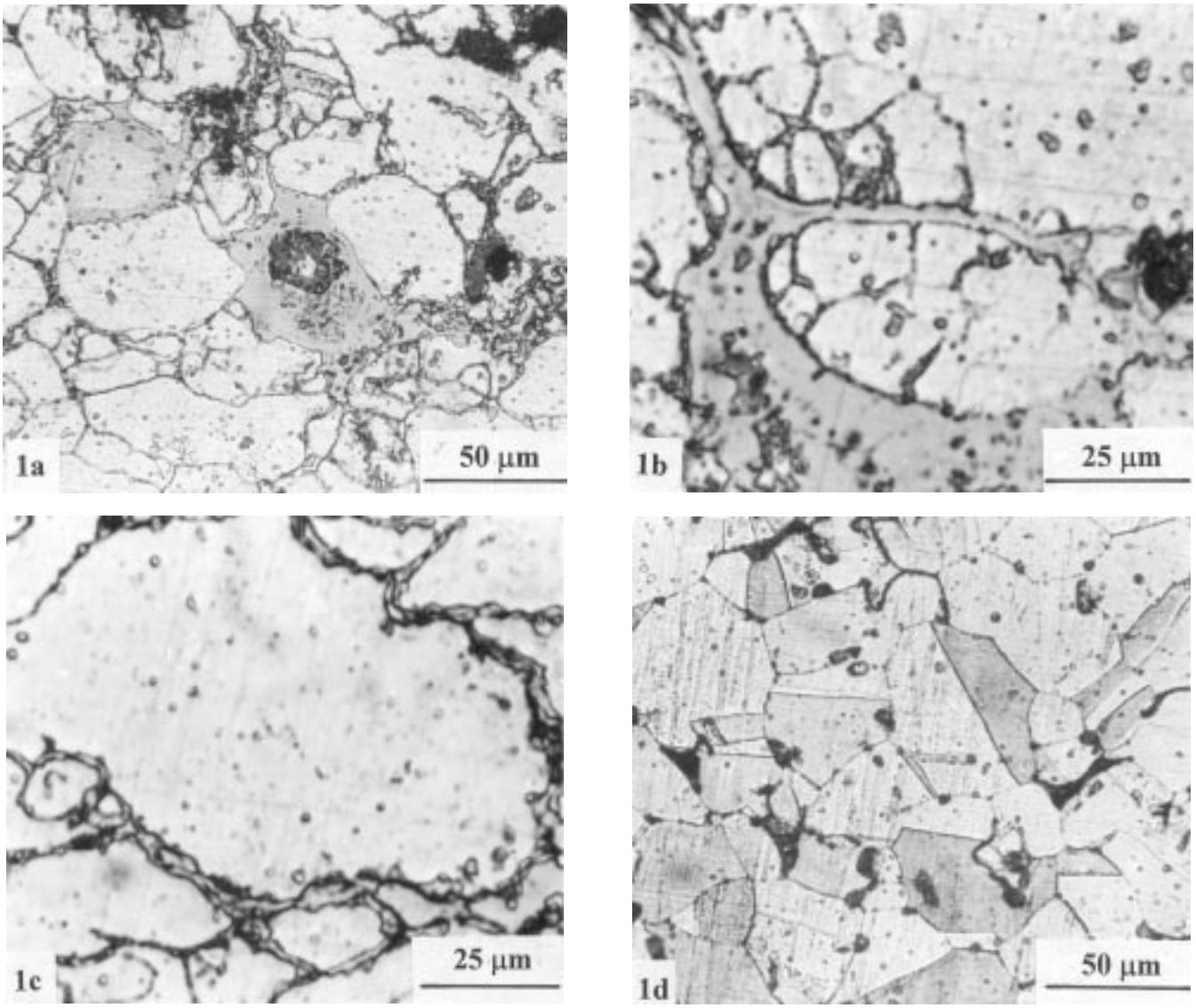

Fig. 1 Microstructure of sintered 304L-Sn alloys. (a) Sintered at 950 °C. (b) Sintered at 1000 °C. (c) Sintered at 1050 °C. (d) Sintered at 1200 °C

found in the study of 316-Sn powder system sintered at 1150 °C for 10 h (Ref 6).

The chemical composition of the austenite matrix and the tin-base liquid phase was measured by electron probe microanalysis (EPMA). For the batch of specimens added with 4 wt% Sn and sintered at 1050 °C, the composition of the matrix was (in weight percent) 18.3Cr-7.6Ni-3.2Sn and iron balance. The composition of the liquid phase was (in weight percent) 15.6Fe-25Ni-2.8Cr and tin balance. During sintering massive atoms of iron, chromium, and nickel dissolved into the tin-base liquid. The nickel showed the highest solubility in the liquid phase in order to reduce the nickel content of the 304L particles from 11 to 7.6 wt%.

3.2 Compact Swelling During Sintering with a Liquid Phase

Figure 2 depicts the variation of volume change ratio of 304L-Sn powder compacts with the tin content and the sintering temperature. For the group of 304L powder specimens the volume shrinkage ratio increased monotonically with increasing sintering temperature. Most of the tin added specimens swelled during sintering. Only 1% addition of tin powder led the compacts to expand when sintered below 1050 °C. The volume expansion ratio increased with an increase in the added tin powder, but decreased with increasing sintering temperature. Typical liquid phase sintering systems such as W-Ni-Cu or W-Ni-Fe (Ref 8) alloy always showed a marked volume shrinkage as the compacts were sintering, but in this study dimensional dilation accompanied the appearance of the tin-base liquid phase. In the investigation of sintering of titanium-aluminum (Ref 9), aluminum-zinc (Ref 10), copper-aluminum (Ref 11), and iron-copper (Ref 12-15) powder mixtures, the volume of these powder compacts increased as the aluminum, zinc, or copper liquid phase appeared.

Table 2 Corrosion potential and passive current density of the 304L-Sn sintered stainless steels in the potentiodynamic polarization measurement

Tin content, wt%	Corrosion potential (*E*), mV	Passive current density (*I*), μA/cm²
0	373	1000
1.0	324	420
1.2	312	195
1.4	297	171
1.6	287	87
1.8	299	166
2.0	316	175

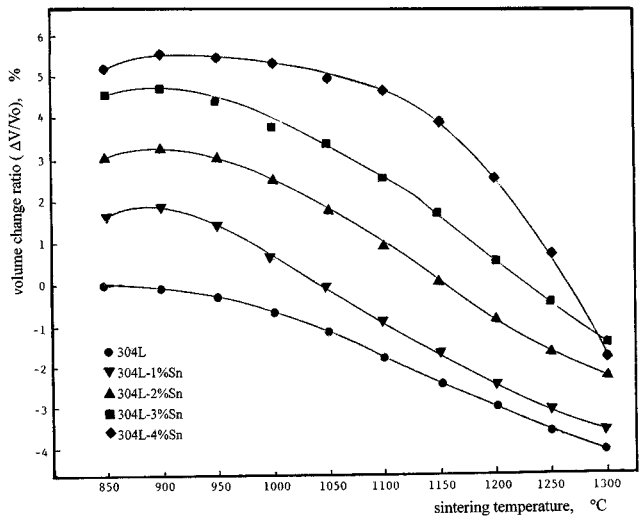

Fig. 2 Variation of volume change ratio of 304L-Sn compacts with the tin content and sintering temperature

The compact swelling during sintering with a liquid phase was mainly attributed to the boundary penetration of solid particles by the liquid phase (Ref 12). From the metallographic examination of Fig. 1(a) to (c) it was found that the tin-base liquid phase can easily penetrate the particle boundaries. As the added amount of tin powder increased, more solid particles were coated with the tin-base liquid, and the thickness of liquid film also increased. This penetration action pushed more 304L particles apart, increased the distance of the particle center, and led to the growth of compacts.

The two mechanisms resulting in compact shrinkage during liquid phase sintering were the particle rearrangement and solution precipitation. In this study the volume percentage of the tin liquid phase was not more than 4%, which was not enough to lead the 304L particles to rearrange to attain a closer packing (Ref 16). For the solution and precipitation mechanism to operate actively, there must be a fairly high solubility of the solid matrix in the liquid phase. As having been over saturated the liquid phase can provide sufficient solute atoms to precipitate on the surface of solid particles. As illustrated in the previous section, the EPMA measurement for the alloys sintered at 1050 °C shows that the composition of liquid phase is (in weight percent) 15.6Fe-25Ni-2.8Cr-0.1Si, respectively. The chromium and silicon content are too low to support the precipitation mechanism to proceed effectively. In other words, it is difficult for the solute atoms to precipitate on the solid particles with a chemical composition similar to that of the 304L matrix (73.2Fe-7.6Ni-18.3Cr-0.9Si, in weight percent). Therefore, the densification mechanism of solution and precipitation cannot operate efficiently. The boundary penetration mechanism dominates the volume change behavior and results in compact swelling during sintering with the tin-base liquid phase.

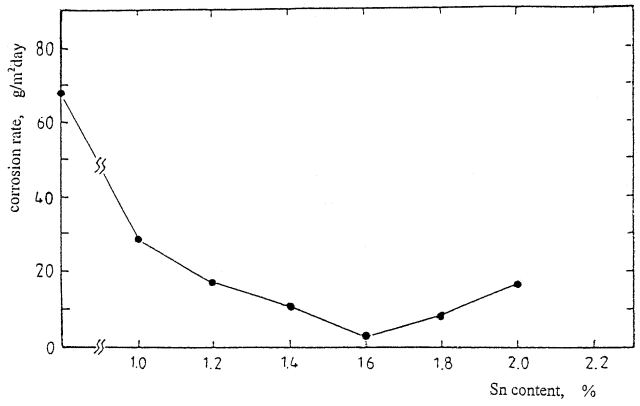

Fig. 3 Variation of the corrosion rate of 304L-Sn alloys sintered at 1200 °C for 40 min with the tin content

3.3 Corrosion Resistance of Sintered 304L-Sn Alloys

Figure 3 depicts the corrosion rate of the alloys sintered at 1200 °C and immersed in 1 *M* H_2SO_4 solution for 576 h as a function of the tin content. The weight loss of sintered stainless steels decreases with increasing tin-added amount, reaches a minimum at the tin content of 1.6 wt%, and then increases. Table 2 illustrates the corrosion potential and the passive current density of potentiodynamic polarization curves. It is shown that both of the measured data reached a minimum for the specimens containing 1.6 wt% Sn powder. Due to the addition of tin powder the anodic reaction of the sintered alloys in 1 *M* H_2SO_4 solution transferred the corrosion potential to a noble value and reduced the corrosion rate. The results of the potentiodynamic polarization measurement are consistent with that of the corrosion rate measurement of the immersion test.

The metallographic examination by scanning electron microscopy (SEM) and the composition measurement by EPMA was conducted on the corroded surface of the 304L-Sn (1.2 wt% Sn) sintered alloys after being immersed in the 1 *M* H_2SO_4 solution for 144 h. It was found that the tin content of pitting spots was about 0.7 wt%, which was lower than the average value (1.2 wt%) of the matrix and grain boundaries. This indicates that pitting is easier to initiate at the area with lower tin content. Therefore, adding tin powder has the beneficial effect of improving the corrosion resistance of the sintered stainless steels.

5. Conclusions

The following conclusions can be drawn:

- Microstructural development of the 304L-Sn powder mixtures during sintering is highly dependent on the sintering temperature. The tin-base liquid phase spreads uniformly among the 304L particles when the sintering temperature is above 1050 °C.
- Compact swelling occurred during sintering as the 304L powder was added with tin powder. The volume shrinkage mechanism of liquid phase sintering, particle rearrangement, and solution precipitation cannot operate effectively. The volume expansion behavior can be ascribed to the boundary penetration of solid particles by the tin-base liquid phase.
- The corrosion resistance of sintered 304L stainless steels in 1 *M* H_2SO_4 solution is improved by adding tin powder. The optimum amount of tin powder to add is 1.6 wt%.

References

1. R. Duckett and D.A. Robins, Effect of Tin Powder Addition on the Sintering Behavior of the Iron Powder, *Powder Metall.*, Oct 1966, p 163-167
2. W.F. Wang and Y.L. Su, Liquid Phase Sintering of Austenitic Stainless Steel Powders with Silicon Addition, *Powder Metall.*, Vol 29 (No. 4), 1986, p 269-275
3. W.F. Wang and Y.L. Su, Mechanical Properties, Corrosion Resistance, and High Temperature Oxidation Resistance of Sintered Duplex Stainless Steels, *Powder Metall.*, Vol 29 (No. 3), 1986, p 177-182
4. A. Tiziani, A. Molinari, L. Fedrizzi, A. Tomasi, and P.L. Bonora, Liquid Phase Sintering of AISI 316L Stainless Steel, *Powder Metall.*, Vol 32 (No. 2), 1989, p 118-122
5. T. Katoh, K. Kusoka, and T. Hisada, Influence of Cu Addition on Some Properties of AISI 304L Stainless Steel Powders, *Met. Powder Rep.*, June 1984, p 351-354
6. S. Harush and D. Itzhak, Hot Pressing and Sintering of Tin-Stainless Steel Metallurgical System, *Powder Metall.*, Vol 31 (No. 3), 1988, p 178-183
7. D. Itzhak and S. Harush, The Effect of Sn Addition on the Corrosion Behavior of Sintered Stainless Steel in H_2SO_4, *Corros. Sci.*, Vol 10 (No. 25), 1985, p 883-888
8. E.G. Zukas and H. Sheinberg, Sintering Mechanisms in the 95%W-3.5%Ni-1.5%Fe Composite, *Powder Technol.*, Vol 13, 1976, p 85-96
9. A.P. Savitskii and N.N. Burtsev, Effect of Powder Particle Size on the Growth of Titanium Compacts during Liquid Phase Sintering with Aluminum, *Soviet Powder Metall. Met. Ceram.*, Vol 20 (No. 9), 1981, p 618-621
10. A.P. Savitskii, N.N. Burtsev, and L.S. Martsunova, Volume Change Experienced by Al-Zn Compacts during Liquid Phase Sintering, *Soviet Powder Metall. Met. Ceram.*, Vol 21 (No. 10), 1982, p 760-764
11. A.P. Savitskii, M.A. Emelyanova, and N.N. Burtsev, Volume Change Exhibited by Cu-Al Compacts during Liquid Phase Sintering, *Soviet Powder Metall. Met. Ceram.*, Vol 21 (No. 5), 1982, p 373-378
12. Y. Wanibe, H. Yokoyama, and T. Itoh, Expansion during Liquid Phase Sintering of Iron-Copper Compacts, *Powder Metall.*, Vol 33 (No. 1), 1990, p 65-69
13. R.L. Lawcock and J.J. Davies, Effect of Carbon on Dimensional and Microstructural Characteristics of Fe-Cu Compacts during Sintering, *Powder Metall.*, Vol 33 (No. 2), 1990, p 147-150
14. K. Tabeshfar and G.A. Chadwick, Dimensional Changes during Liquid Phase Sintering of Fe-Cu Compacts, *Powder Metall.*, Vol 27 (No. 1), 1984, p 19-24
15. S.J. Jamil and G.A. Chadwick, Investigation and Analysis of Liquid Phase Sintering of Fe-Cu and Fe-Cu-C Compacts, *Powder Metall.*, Vol 28 (No. 2), 1985, p 65-71
16. F.V. Lenel, Powder Metallurgy—Principles and Applications, Vol 225, 1980, Metal Powder Industries Federation